A. Saint-Jalmes, S. J. Cox, S. Marze, M. Safouane, D. Langevin, D. Weaire

Experiments and Simulations of Liquid Imbibition in Aqueous Foams under Microgravity

We describe the capillary motion of liquid into aqueous foams under microgravity. Experiments in which a constant input of liquid is added to a foam under a variety of controlled experimental conditions (bubble size, cell geometry, bubble interfacial properties) have been performed in parabolic flights and in the MAXUS 6 sounding rocket. For comparison, we also performed numerical simulations, based on the foam drainage equations in which the gravitational contributions are removed. The agreement between these simulations and the experimental data is good, and the quantitative adjustment between them enables us to estimate foam permeabilities and surface shear viscosities.

Authors

A. Saint-Jalmes, S. Marze, M. Safouane, D. Langevin
Laboratoire de Physique des Solides
Université Paris-Sud
91405 Orsay, France.

S. J. Cox
Institute of Mathematical and Physical Sciences
University of Wales
Aberystwyth, SY23 3BZ, UK

D. Weaire
Department of Physics
Trinity College
Dublin 2, Ireland.

Correspondence

Dr. A. Saint-Jalmes,
saint-jalmes@lps.u-psud.fr,
Tel +33 1 69 15 69 60
Fax + 33 1 69 15 60 86

1. Introduction

On the ground, aqueous foams evolve irreversibly, mainly because of a gravity-induced effect (called drainage), which tends to separate gas and liquid [1-3]. This drainage prevents the investigation of foams containing large liquid volumes (typically more than 10%), as well as longtime studies. In microgravity (μg) conditions, the gravitational drainage disappears and the foam liquid fraction becomes constant in time. A "FOAM" module for the ISS is now under development under the supervision of ESA (details on its principles, goals and methods are given in [4]). It will be dedicated to study foam structure, rheology, stability, and coarsening. Within the FOAM preparation process, we have performed three Parabolic Flight (PF) campaigns (ESA 34th, 35th and 37th campaigns) in collaboration with EADS-ST at Friedrichshafen, and have also flown an experimental module in the MAXUS 6 sounding rocket (launched in Nov. 04, and developed both by EADS-ST and SSC). During these flights, we performed liquid imbibition experiments, studying how liquid is transported within the foam liquid matrix due to capillary effects. The goal of such imbibition experiments, either on ground or in microgravity, is to scan and understand the foam structure and its finest details : the way the liquid propagates into the foam results from subtle balances between bulk and interfacial flows [2,3,5], and depends on the bubble geometry and on the liquid distribution between the different parts of liquid structure (channels, nodes and films [1-5]). The interest in performing such experiments in microgravity is to have access to new situations with wet foams (which are impossible to observe on ground [6-7]), and to have a different driving force on the liquid (capillary rather than gravitational). In the same time, a strong analytical and numerical work has also been applied to this issues [8]. In this paper, we present some of these imbibition results and corresponding simulations, and discuss the agreements.

2. Experiments: concepts, setup and hardware

Starting with a dry homogeneous foam, a forced imbibition (or wetting) experiment consists of injecting some surfactant solution (the same as the one used to make the foam) at a given location and at a controlled flow rate, and simultaneously following how this liquid propagates into the foam [1]. The propagation is due to capillarity which tends to transport liquid from wet parts of the foam to drier ones, and to smooth out gradients in the liquid fraction [1-5,8]. In comparison with previous attempts in µg [9-10], these experiments are the first with 3D foams, and in which the bubble size, foam homogeneity, polydispersity, and the injection rate are controlled. We used different geometries and initial conditions for the PF and for MAXUS, especially tuning the bubble size to scale the experiment timescale to the available µg time.

In the PF experiments, the foams are made by bubbling some air into the surfactant solution during the normal gravity phases: this provides us with a foam of bubble diameter $D = 3.2$ mm, large enough to get measurable liquid propagation during the 20s of µg. The initial liquid fraction is $\varepsilon_0 \approx 0.1\%$. As shown in Fig. 1(a), the foam is inside a transparent rectangular cell (height = 30 cm, width = 10 cm and thickness = 3 cm): liquid is injected at one side of the cell ($x = 0$), at a constant rate Q (varied between 10 to 55 mL/min), and evenly spread across the whole cross section. Macroscopically, the liquid can thus only propagate in the x direction (1D macroscopic propagation). Nevertheless, the foam itself is 3D, with about 10 bubbles across the thickness of the cell: this is enough to obtain a multiple scattering of light by the foam [11], and to use white light transmission to detect liquid fraction variations and liquid front positions [4,11,12]. Note that due to undesirable shadows from the cell edges, no measurements can be done for $x < 2.5$ cm.

In the MAXUS rocket experiment, within the whole flight timeline and the different tests, the µg time dedicated to the imbibition experiment was 350s. Only one flow rate was studied, with continuous injection during 150s, followed by 200s in which the liquid is allowed to rearrange within the foam. The cell geometry and foam properties in MAXUS are chosen to mimic the ones foreseen for the ISS, where imbibition and rheological experiments have to be done in a single cell [4]. For the cell type, we use a flat cylindrical "cone –plate" geometry, usual for rheological measurements (with the cone able to rotate to shear the sample). Fig. 1b shows a side view, with vertical symmetry axis z. The cell outer radius is 7cm, and the height at its edge is 1cm. For the imbibition experiment, the cone part is fixed, and the liquid is injected from below at the cell center, thus propagating in the radial direction r. In order to have a 3D sample within the small cone-plate gap, the foam production device used in MAXUS provided bubbles of diameter $D \approx 300\mu m$ [13]. The initial liquid fraction is 5%, and its variations with time and along the cell radius are measured by a set of electrodes, facing each other (Fig. 1b). The foam electrical conductance is measured, and is proportional to the liquid fraction [1,14]. The PF experiments correspond to 1D propagation, while in MAXUS we have a situation between a 2D (if the distance between the two cell sides were constant) and a 3D propagation.

For all the experiments reported here, the same surfactant solution is used: a mixture of Sodium Dodecyl Sulfate (SDS) at a concentration $c = 8$g/L, and dodecanol (DOH), at a concentration $c = 0.1$ g/L. This implies high surface shear viscosities, and thus low surface mobilities [5].

Starting from the usual drainage equations [1-3], those describing time and position variations of the liquid fraction with $g = 0$ have been recently discussed for different imbibition

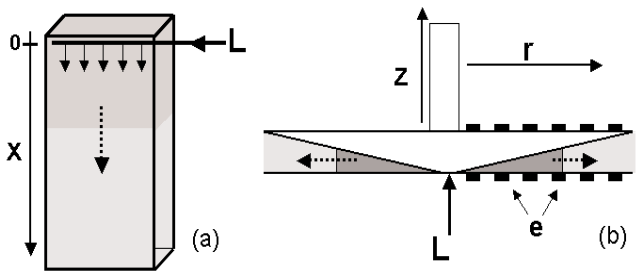

Fig. 1: Experimental geometries : (a) rectangular cell with injection of liquid (L) at x = 0, (parabolic flights); (b) the "cone-plate" cell, with electrodes (e), and injection at the center r = 0 (MAXUS 6 rocket). Foams appears in grey (light for the dry part, and dark for wetted part). The dashed arrow show the direction of liquid propagation.

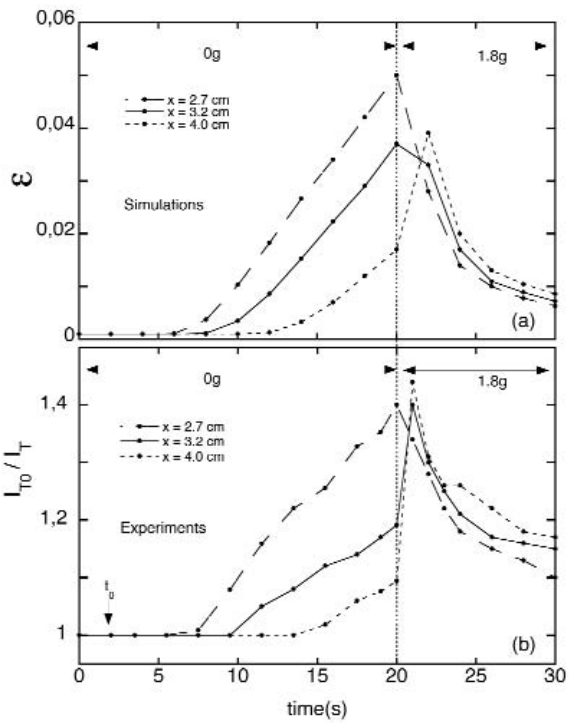

Fig. 2: PF experiments : (a) numerical calculations of the liquid fraction ε, at three different positions; (b) normalized transmitted intensity at the same three different positions in the experiments.

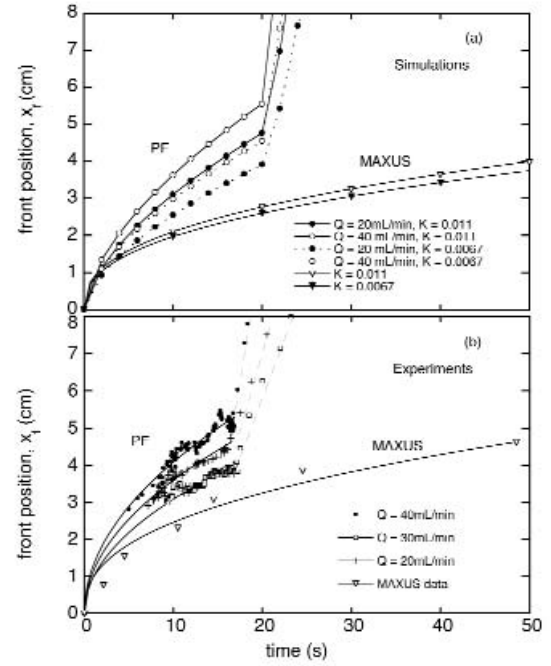

Fig. 3: Front positions as a function of time: (a) numerical calculations and (b) experimental results.

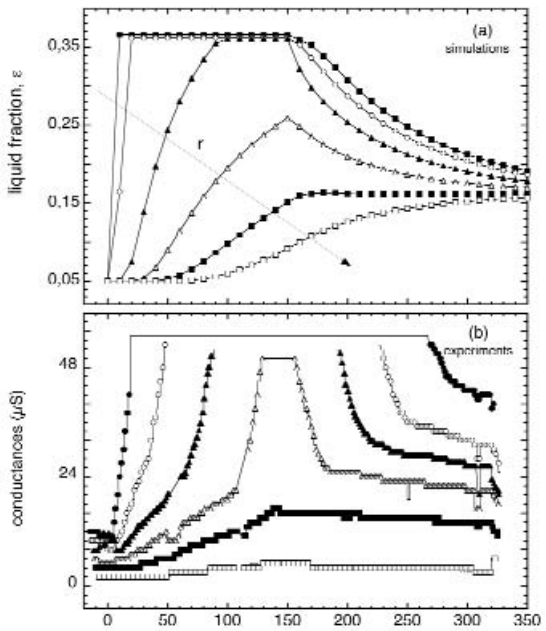

Fig. 4: MAXUS experiments : for the same radii, (a) numerical calculations of the liquid fraction ε (for K = 1/150) and (b) time evolution of the electrical conductances in the experiments. Liquid injection stops at t = 150s. For a given, r when ε reaches and saturates at 0.36, it means that only pure liquid is found at r (as also found in the experiments).

types, geometries, surface mobilities, etc... [8]. Some analytical predictions are available. For instance, the front position x_f in the limit of low surface mobility is

$$x_f \sim K^{2/(d+4)} Q^{1/(d+4)}\, t^{3/(d+4)}$$

where d is the macroscopic dimension associated to the propagation, K is the foam permeability [2-5], Q is the injected flowrate, and t the time. However, in most cases, solving the equations requires numerical simulations, especially if one wishes to take into account the details of the experimental conditions. Here, resolutions of the $g = 0$ differential drainage equations shown in [8] are made in the limit of small surface mobilities (as expected for the experiments), and the permeability K is taken as the only free parameter.

3. Parabolic Flight results

We first present experimental results for the PF experiments, and the associated simulations. The time evolution of the liquid fraction ε, calculated at three different distances x from the injection, is plotted in Fig. 2a. For the same positions, Figure 2b shows the time evolution of the transmitted intensity ratio I_{t0}/I_t, which is proportional to the liquid fraction, (with I_{t0} the transmitted intensity at $t = 0$). Note that the injection starts at $t = 0$s in the simulation, but only at $t = t_0 = 2$s in the experiments. In the 0g phase, it is clear that the curves are qualitatively very similar in both figures: one can see that the liquid propagates into the foam, and that the way the liquid content rises at a given x is identical and linear in both experiments and simulations, and independent of x. Once in hypergravity, most of the injected liquid which remained close to the foam top falls down as a sharp and very fast pulse. Experimentally and numerically, it travels through the foam down to roughly $x = 5$cm in about 1s. This is why it is hardly seen in Fig.2a, where calculations are made every 2s, and more clearly detected in Fig. 2b (see the peak for $x = 4$cm) where points are measured at shorter intervals. Nevertheless, at long times, the foam drainage (decay of the pulse tail) is again identical in both figures.

At a given time t, the liquid fraction decreases with x, down to x_f where the initial value is recovered. This defines a liquid front position $x_f(t)$, corresponding to the maximum distance reached by the liquid at t. In Fig. 3a, we have plotted numerical results for two different flowrates Q, and two different values of the permeability K. In fact, $K = 1/150$ (≈ 0.0067) is the theoretical value for perfectly immobile surfaces, whereas some mobile surfaces have a higher value of K [5]. The bubble size, surface tension and cell size correspond to those of the experiments, as well as the initial liquid fraction $\varepsilon_0 = 0.1\%$. For this figure, the front is associated with the position at which the liquid profile reaches $\varepsilon_f = 0.2\%$, slightly above ε_0. This is chosen to mimic the experimental detection method and its accuracy: it

is actually possible, with the light scattering method and in the case of dry foams, to detect tiny variations of ε above ε_0, so we believe that the measured front must correspond to a liquid fraction ε_f just slightly above ε_0.

Looking at the simulations, it first appears that they are in agreement with the analytical scaling for the front position given before, confirming for instance a power law $\alpha = 3/5$ for the time dependence, and the small dependence on flow rate, $Q^{1/5}$. This is not surprising because the situation with $\varepsilon_0 = 0.1\%$ and $\varepsilon_f = 0.2\%$ is close to the analytical case $\varepsilon_0 = \varepsilon_f = 0$. To compare with the experiments, it is possible to scale the simulations to fit the data (solid lines for t < 20s in Fig. 3b), providing a best fit value for K, for all flowrates. Adjusting the simulations in this way gives a permeability $K = 0.01$. This implies a surface mobility parameter $M = 0.15$ [5], which is small as expected. From this M we can deduce the surface shear viscosity, $\mu_s = 1.1\ 10^{-3}$ g.s^{-1}, knowing bubble size and bulk viscosity [5] ; this value is in very good agreement with ground measurements on similar solutions, and confirms the validity of the adjustment in Fig. 3b. Finally, in the 1.8g phase, it is found in both simulations and experiments that the front position increases linearly and very quickly with time.

4. MAXUS results

For the MAXUS experiments, similar comparisons can be done. First, we examine qualitatively the time evolution of the liquid fraction at different radii (Fig. 4). In the simulations, one can see that the liquid fraction increases during injection, followed by a redistribution of liquid once the injection is stopped at $t = 150$s, which tends to evenly redistribute the liquid. The experimental curves of conductance in Fig. 4b show very similar trends. Note that close to the center of the cell the simulations show that the liquid fraction increases rapidly, and gets so high that locally there is no longer a foam, but a pool of pure solution is formed (this occurs as soon as ε reaches 36%, corresponding to a sharp foam-liquid interface [1-3]). Experimentally, video observations confirmed the occurrence of this pure liquid pool, in agreement with the saturation of the conductance value, and never observed on ground as convective instabilities prevent to access to such high ε [6-7]. After the injection is stopped, the liquid pool in the center vanishes, as its liquid is redistributed into the foam.

Fig. 3a also reports calculations of the front position for the MAXUS conditions, with ε_0 =5%, assuming again a good experimental accuracy so that $\varepsilon_f = 5.1\%$. Power-law fits provide an exponent $\alpha_{sim} \approx 0.4$, which seems closer to the analytical predictions for $d = 3$ ($\alpha = 3/7$) than to $d = 2$ ($\alpha = 1/2$). Note though that the difference between such close exponents is difficult to detect, and that $\varepsilon_f = 0$ in the analytical model. As shown in Fig. 3b, the MAXUS data can also be adjusted by a power law, and a same exponent 0.4 is found. From this power-law best fit, one gets $K = 0.011$, again in good agreement with results already found for such small bubbles [5].

5. Conclusions

We have successfully performed imbibition experiments in aqueous foams under µg: for various experimental conditions, we have been able to measure the propagation features. Comparisons between experiments and simulations show that the drainage equation with $g = 0$ actually well describes all the observed features, especially the front propagation is quantitatively in close agreement with the predictions.

6. Acknowledgements

The authors thank ESA for financial support through the MAP program.

References

[1] *D. Weaire and S. Hutzler.* 1999. The Physics of Foams. Clarendon Press, Oxford.

[2] *S.J. Cox, D. Weaire, S. Hutzler, J. Murphy, R. Phelan and G. Verbist.* 2000. Applications and generalizations of the foam drainage equation. Proc. R. Soc. Lond. A. 456: 2441 – 2464.

[3] *S. A. Koehler, S. Hilgenfeldt and H. A. Stone.* 2000. A generalized view of foam drainage: experiments and theory. Langmuir 16: 6327 – 6341.

[4] *A. Saint-Jalmes, S. Marze, M. Safouane, D. Langevin.* 2006. Foam experiments in parabolic flights. Microgravity Sci. Technol. 18 : 5-13

[5] *A. Saint-Jalmes, Y. Zhang and D. Langevin.* 2004. Quantitative description of foam drainage : transitions with surface mobility. Eur. Phys. J. E. 15: 53-60.

[6] *S. Hutzler, D. Weaire and R. Crawford.* 1998. Convective instability in foam drainage. Europhys. Lett. 41: 461 – 465.

[7] *M.U. Vera, A. Saint-Jalmes and D.J. Durian.* 2001. Instabilities in a liquid fluidized bed of gas bubbles. Phys. Rev. Lett. 84: 3001 – 3004.

[8] *S.J. Cox and G. Verbist.* 2003. Liquid flow in foams under microgravity. Microgravity Sci. Technol. 14: 45 – 52.

[9] *D. Noever and R.J. Cronise.* 1994. Weightless bubble lattices: a case of froth wicking. Phys. Fluids. 6: 2493 – 2500.

[10] *H. Caps, H. Decauwer, M.-L. Chevalier, G. Soyez, M. Ausloos, and N. Vandewalle.* 2003. Foam imbibition in microgravity. Eur. Phys. J. B. 33: 115 - 119 ; H. Caps, S.J. Cox, H. Decauwer, D. Weaire, N. Vandewalle. 2005. Capillary rise in foams under microgravity. Colloids Surfaces A. 261: 131 - 135.

[11] *M.U. Vera, A. Saint-Jalmes and D.J Durian.* 2001. Scattering optics of foam. Applied Optics. 40: 4210 – 4216.

[12] *A. Saint-Jalmes, M.U. Vera and D.J. Durian.* 2000. Free drainage of aqueous foams : container shape effects on capillarity and vertical gradients. Europhys. Lett. 50: 695 – 701.

[13] *S. Marze, A. Saint-Jalmes, D. Langevin, S.J. Cox, D. Weaire.* 2005. Foam experiments in the Maxus 6 sounding rocket : development towards the ISS foam module. Proceedings of the 17th ESA symposium on European rockets and balloons, ESA SP-590.

[14] *K. Feitosa, S. Marze, A. Saint-Jalmes, D. J. Durian.* 2005. Electrical conductivity of dispersions : from dry foams to dilute suspensions. J. Phys. Cond. Matter 17 : 6301-6305